



HAL
open science

Quantitative analysis of the formation of monodisperse cello-oligomers obtained by phosphoric acid hydrolysis

Noriyuki Isobe, Yuko Ono, Yoshiharu Nishiyama, Denis Roux, Akira Isogai

► To cite this version:

Noriyuki Isobe, Yuko Ono, Yoshiharu Nishiyama, Denis Roux, Akira Isogai. Quantitative analysis of the formation of monodisperse cello-oligomers obtained by phosphoric acid hydrolysis. *Cellulose*, 2023, 30, pp.8235-8243. 10.1007/s10570-023-05415-1 . hal-04177453

HAL Id: hal-04177453

<https://hal.science/hal-04177453v1>

Submitted on 4 Aug 2023

HAL is a multi-disciplinary open access archive for the deposit and dissemination of scientific research documents, whether they are published or not. The documents may come from teaching and research institutions in France or abroad, or from public or private research centers.

L'archive ouverte pluridisciplinaire **HAL**, est destinée au dépôt et à la diffusion de documents scientifiques de niveau recherche, publiés ou non, émanant des établissements d'enseignement et de recherche français ou étrangers, des laboratoires publics ou privés.



Distributed under a Creative Commons Attribution 4.0 International License



Quantitative analysis of the formation of monodisperse cello-oligomers obtained by phosphoric acid hydrolysis

Noriyuki Isobe · Yuko Ono ·
Yoshiharu Nishiyama · Denis Roux ·
Akira Isogai

Received: 31 March 2023 / Accepted: 18 July 2023
© The Author(s) 2023

Abstract Hydrolysis of cellulose in concentrated phosphoric acid is known to give two distinctive mono-disperse cello-oligomers: the degree of polymerization (DP) of 7 and 15. To understand the formation mechanism of monodisperse cello-oligomers, the transition of DP during phosphoric hydrolysis was monitored by size-exclusion chromatography combined with multiangle laser-light scattering analyses (SEC/MALLS). The obtained results suggested that

not the hydrolysis at a specific length but random hydrolysis was likely. The rate of hydrolysis slowed down when the DP reached around 40, and the pool of cello-oligomers appeared at the incubation of 35 days. Then, the mono-disperse cello-oligomers were recovered from the pool of cello-oligomers by fractionation based on the solubility difference.

Keywords Cellulose oligomers · Phosphoric acid hydrolysis · SEC-MALLS

Supplementary Information The online version contains supplementary material available at <https://doi.org/10.1007/s10570-023-05415-1>.

N. Isobe
Research Institute for Marine Resources Utilization (MRU), Japan Agency for Marine-Earth Science and Technology (JAMSTEC), 2-15 Natsushima-cho, 237-0061 Yokosuka, Kanagawa, Japan

N. Isobe (✉) · Y. Ono · A. Isogai
Department of Biomaterial Sciences, Graduate School of Agricultural and Life Sciences, The University of Tokyo, 1-1-1 Yayoi, Bunkyo-ku, Tokyo 113-8657, Japan
e-mail: isoben@jamstec.go.jp

Y. Nishiyama
Centre de Recherches sur les Macromolécules Végétales (CERMAV), Centre National de la Recherche Scientifique (CNRS), Univ. Grenoble Alpes, 38000 Grenoble, France

D. Roux
Laboratoire Rhéologie et Procédés, Université Grenoble Alpes, Grenoble INP, CNRS (UMR 5520), Domaine Universitaire, BP 53, Grenoble, France

Introduction

Oligosaccharides are an important class of biomaterials with a wide range of applications. Biologically, oligosaccharides serve as recognition or adhesion sites on living cells and are considered to have biological activities and potential therapeutic effects (Muanprasat and Chatsudthipong 2017). In addition, oligosaccharides have been used as a model compound for polysaccharides: the single crystals of cello- or chito-oligomers give the essential information of cellulose and chitin crystal structures (Buleon and Chanzy 1978; Cartier et al. 1990; Persson et al. 1992; Helbert and Sugiyama 1998). In particular, Chanzy and co-workers clearly showed the chain orientation within the crystals based on the electron micrographs and electron diffraction diagrams on the single crystals made of cellulose, chitin, and chitosan oligomers (Buleon and Chanzy 1978; Cartier

et al. 1990; Persson et al. 1992; Helbert and Sugiyama 1998). Moreover, oligosaccharides are the building block for designable materials. Maltoheptaose (amylo-oligomer) serves as the hydrophilic domain in block copolymer that self-assembles into a highly ordered structure with periodicity on the nanometer scale (Cushen et al. 2012). Cello-oligomers can form nanoribbon structure, the surface functional groups of which are modifiable (Yataka et al. 2015; Serizawa et al. 2017).

In general, oligosaccharide preparation is classified into three paths: (i) chemical synthesis (Seeberger 2008; Oscarson and Cheallaigh 2021; Fittolani et al. 2022), (ii) enzymatic synthesis with glycosyl transferases or glycosidases (Perugino et al. 2004; Hiraishi et al. 2009; Hata et al. 2018), and (iii) scission of polysaccharides (Isogai and Usuda 1991; Meiland et al. 2011). While chemical and enzymatic synthesis can achieve desirable and complicatedly branched oligosaccharides, a simple short-chain and non-branched oligosaccharide can be prepared by scission of polysaccharides. As such, acid hydrolysis was well established. Specifically, phosphoric acid hydrolysis is known for its unique nature: it gives two distinctive lengths of cello- (and chito-) oligomers, degree of polymerization (DP) of 7 and 15 (Isogai and Usuda 1991; Helbert and Sugiyama 1998; Zhang et al. 2021). Briefly, cellulose is dissolved in 83 wt% phosphoric acid and the solution is incubated at room temperature for more than 4 weeks. Then, by diluting the solution with water, precipitation takes place. The precipitates contain cello-oligomer of DP 15 and the supernatant contains DP 7 that is recovered by the subsequent addition of methanol. Despite the simple and environmentally-benign aqueous process, the time-course reaction is a mystery, and therefore the mechanism behind the formation of DP 7 and 15 remains unclear, leading to the unsuccessful preparation of mono-disperse cello-oligomers (Meiland et al. 2011). To mitigate this, it is crucial to understand how DP changes in the course of the reaction.

For this aim, size-exclusion chromatography combined with multiangle laser-light scattering analyses (SEC/MALLS) is suitable. SEC/MALLS is the technique that combines the fractionation of solute molecules by chromatography and the measurement of absolute molecular mass by multiangle light scattering. One of the great advantages of SEC/MALLS is the quantitative nature. By using the accurate

refractive index increment (dn/dc), the mass calculated from the integration of SEC elution curves corresponds to the injected mass (Ono et al. 2016). In addition, the absolute molar mass is given to each slice of SEC elution curves by MALLS. Consequently, the absolute molar mass can be given to all the injected molecules, as long as all the injected molecules are completely dissolved in the eluent; this is the case for the easy-dissolving cello-oligomers.

Here, the time-course change in DP during phosphoric acid hydrolysis was monitored in a quantitative manner: By multiplying the yield of phosphoric acid hydrolysis to the SEC elution curves, one can discuss which and how much fraction appears and disappears in the course of incubation. Through the transition of DPs, the mechanism behind the formation of mono-disperse cello-oligomer obtained by phosphoric acid hydrolysis was speculated.

Materials and methods

Materials

Microcrystalline cellulose powder (Funacell, Funakoshi, Japan) was used as a starting cellulose. Phosphoric acid, methanol, and acetone (FUJIFILM Wako Pure Chemical, Japan) were used without further purification. Deuterated DMAc (DMAc-d₉) was purchased from Cambridge Isotope Laboratories (Massachusetts, USA). Deionized water was used in this study.

Phosphoric acid hydrolysis

Phosphoric acid hydrolysis was performed according to Isogai and Usuda (1991). Cellulose powder (22.25 g) was added in 683.46 g of 85% H₃PO₄ and 16.0 g of water and incubated at room temperature. To facilitate the dissolution, the undissolved portion of cellulose was smashed with a glass rod. The solution became completely transparent 2 days after the start of incubation. At 7, 14, 21, 28, 35, and 42 days from the start of incubation, 102 g of solution was taken. The half portion (51 g) was poured into 500 mL of water, leading to the precipitation. The precipitation was washed with water by centrifugation until it showed neutrality, and then washed with acetone to the remove brownish color. This insoluble

fraction was denoted as “Fraction A”. The supernatant was poured into 1 L of methanol, and the precipitation was recovered by centrifugation and washed with water until it showed neutrality. This soluble fraction was denoted as “Fraction B”. In addition, the other portion (51 g) was poured into 500 mL of methanol, leading to precipitation. The precipitation was washed with water by centrifugation until it showed neutrality, and then washed with acetone to remove the brownish color. This insoluble fraction was denoted as “Fraction all”.

SEC-MALLS

The SEC/MALLS analysis system comprising SEC columns (KD-806 M and KD-802, Shodex, Japan), a MALLS detector (DAWN HELEOS-II, $\lambda = 658$ nm, Wyatt Technologies, USA), and 1.0% w/v LiCl/DMAc was used as an eluent. Other SEC attachments and the operation conditions are described elsewhere (Ono et al. 2016).

NMR

The ^{13}C NMR spectra were recorded at 23 °C using a JMN-ECA II 500 spectrometer (JEOL, Japan). Deuterated DMAc (0.525 ml) was added to 0.075 mL of 8% LiCl/DMAc with cello-oligomer concentration of 0.291 mg/ml.

Results and discussion

Characterization of mono-disperse cello-oligomers

Phosphoric acid hydrolysis of micro-crystalline cellulose powder was conducted according to Isogai and Usuda (Fig. 1a) (Isogai and Usuda 1991), where Fraction A and B after 6 weeks of incubation were reported to have weight-average DP (DP_w) 15 and 7, respectively. Other than the monodisperse cello-oligomers, un-fractionated acid hydrolyzed products “Fraction all” were recovered by the addition of methanol into cellulose/phosphoric acid solution in order to examine if the additional hydrolysis took place upon the dilution with water (“Addition of water” in Fig. 1a). The yields of Fraction all decreased monotonically (Fig. 1b), indicating that a certain amount (up to 350 mg per 1 g input of cellulose) became water-soluble in the form of water-soluble cello-oligomers (DP: less than 6) (Taylor 1957) or furfurals, and was washed away during the washing step. While the yield of Fraction A decreased, that of B increased and reached a plateau.

To confirm that the hydrolyzed products were cello-oligomers, ^{13}C NMR was performed (Fig. 2). The spectra of both Fraction A and B were in accordance with that of reported cello-oligomers (Isogai 1997). Although the existence of a small amount of phosphorous (around 0.13 at% at a maximum) in the form of phosphate was reported

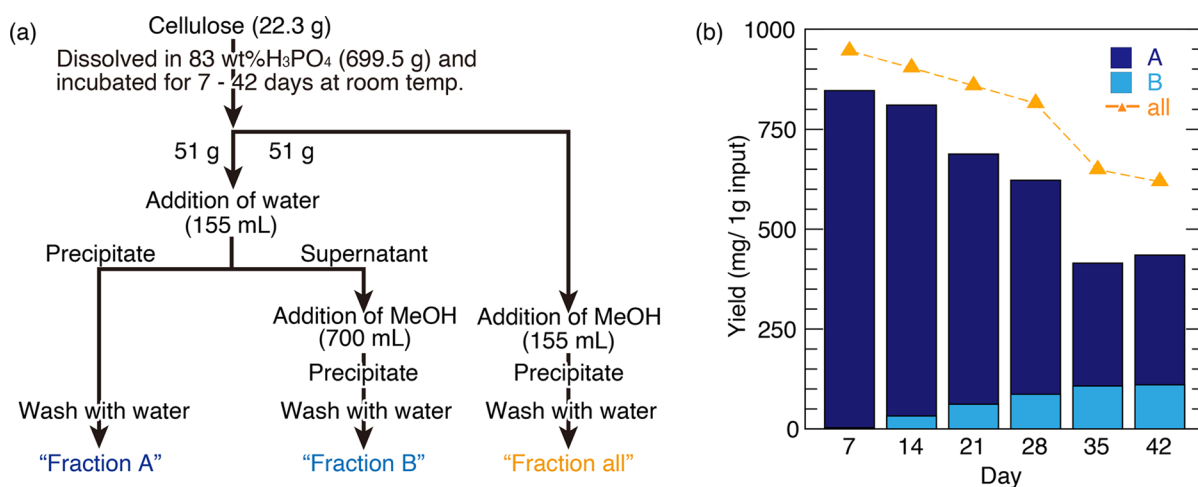


Fig. 1 **a** Preparative scheme of cello-oligomers, **b** yields of Fraction A, B, and all, which were obtained by dividing the mass of each fraction (Fraction A, B, and all in **a**) with the initial input of starting cellulose powder (22.3 g)

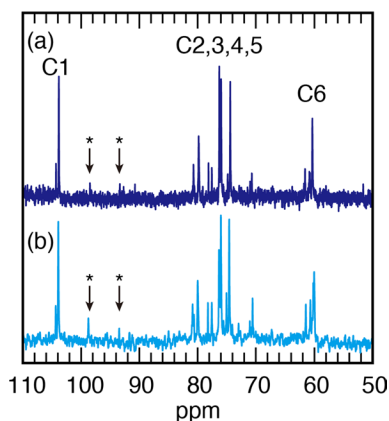


Fig. 2 ^{13}C NMR spectra of (a) Fraction A and (b) B recovered at 35 days of incubation. Asterisks show epimer at the C1 of reducing end

(Jiang et al. 2021), ^{13}C NMR did not detect any phosphate-related signals. By the ratio of the area of two peaks, namely C1 participating in β -1,4 glucosyl bond and C1 at the reducing end, the number average DPs was calculated: 11.2 for Fraction A and 5.1 for Fraction B, which were in accordance with the reported DPs, 15 and 7. Therefore, the hydrolyzed cellulose obtained by phosphoric acid was purely cello-oligomers as reported.

To monitor the transition of DPs, SEC/MALLS was performed on Fraction A and B (Fig. 3; Table 1). At 7 days of incubation, the molar mass distribution of Fraction A (Fig. 3a) was broad (dispersity, \bar{D} : 1.6) and centered at around 5000–6000, namely DP 30–40 (DPw: 37). As the incubation time proceeded, the distribution became narrower (\bar{D} changed from 1.6 to 1.2), and the peak center shifted to molar mass of 2000–3000, namely DP 12–18 (DPw: 15.4). In contrast, the molar mass distribution of Fraction B (Fig. 3b) was sharp from the first appearance at 14 days incubation (\bar{D} : 1.3), and the peak center did not change (DPw: 8). The constantly mono-disperse nature of Fraction B (DPw: 8) should arise from the water solubility of cello-oligomers with the DP less than 6 (Taylor 1957) that were washed away during the washing step (Jiang et al. 2021; Zhang et al. 2021). As a result, the origin of mono-disperse nature of DP 15 (Fraction A) needs to be addressed.

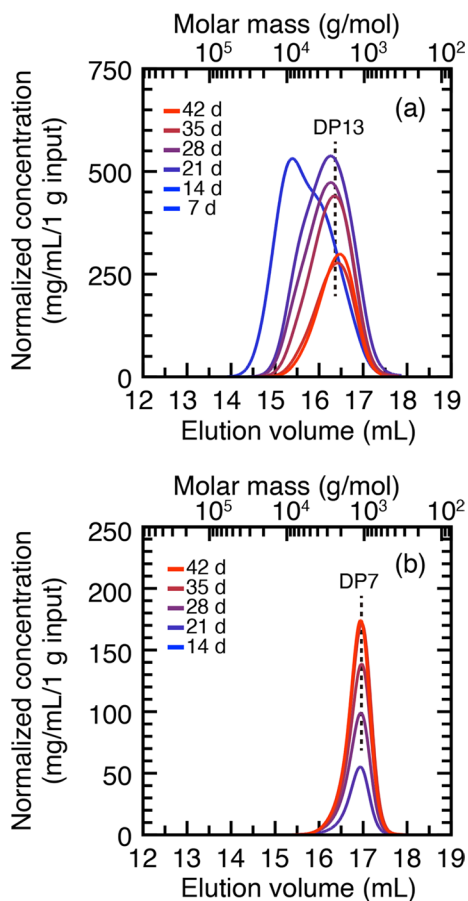


Fig. 3 SEC/MALLS elution patterns of (a) Fraction A and (b) B. Incubation periods are shown in the figures. Normalized concentration (mg/mL/1 g input) was the concentration normalized by the yields as detailed in Supporting Information so as to visualize the transition of DPs and yields of each fraction. Molar mass at each elution volume is also shown on top of figures for clarity

Effect of addition of water on the oligomer formation

One possible explanation for the formation of mono-disperse nature of DP15 is the hydrolysis at a specific length during the precipitating step; namely, the highly crystalline aggregates of cello-oligomers are formed during the precipitating step (“Addition of water” in Fig. 1a) and the edge of crystals is susceptible to the further hydrolysis induced by the additional water. Indeed, the yield of Fraction A+B did not correspond to Fraction all in Fig. 1b, indicating that the addition of water in the precipitation step caused the additional hydrolysis, leading to the formation of

Table 1 The yields, weight-average DP (DP_w), and dispersity (\bar{D} = DP_w/DP_n) of each fraction

Time (day)	Fraction A			Fraction B		
	Yield (mg/1 g input)	DP	\bar{D}	Yield (mg/1 g input)	DP	\bar{D}
7	843.4	37.7	1.6	2.8	N/A	N/A
14	778.2	22.8	1.3	32.4	8.0	1.3
21	626.5	20.4	1.3	61.8	8.6	1.2
28	535.7	17.3	1.2	86.7	8.0	1.2
35	307.6	16.7	1.2	107.5	8.0	1.2
42	324.9	15.4	1.2	110.3	8.0	1.1

Yields of Fraction A and B were obtained by dividing the mass of each fraction with the initial input of starting cellulose powder (22.3 g)

additional water-soluble cello-oligomers that were lost during the subsequent washing step. To examine the possibility of specific hydrolysis during precipitating step, the SEC-MALLS elution profiles of Fractions all, A, and B were compared in Fig. 4. Owing to the above-mentioned quantitative nature of SEC-MALLS, one can add the elution profiles of Fractions A and B, and compare it with Fraction all. Both at 14 and 42 days of incubation period, the peak position and the shape of elution profiles were largely identical between Fractions all and A+B, showing that the random hydrolysis took place at the precipitating step.

Scission probability

Another possible explanation of the mono-disperse nature of DP15 (Fraction A) is the hydrolysis at a specific length. To examine this, the analysis of Fraction all that contains all hydrolyzed products other than water soluble cello-oligomers is beneficial. If the specific hydrolysis takes place, DP15 will appear from the beginning of hydrolysis. As seen in Fig. 5a, the elution patterns of Fraction all were broad and contained several species. To deconvolute these patterns including overlapping distributions, the second derivatives are powerful (Fig. 5b) (Talsky et al. 1978). In the second derivatives, the peak position appears as a downward concave as indicated with arrows in Fig. 5b. In the starting cellulose, there were two downward concaves centered at 14.8 mL (Species 1) and 16.0 mL (Species 2), with corresponding DPs of 170 and 30, respectively. As the incubation proceeded from 7 to 28 days, the two concaves of Species 1 and 2 gradually shifted to larger elution volume and another downward concave centered at 17.0 mL (Species

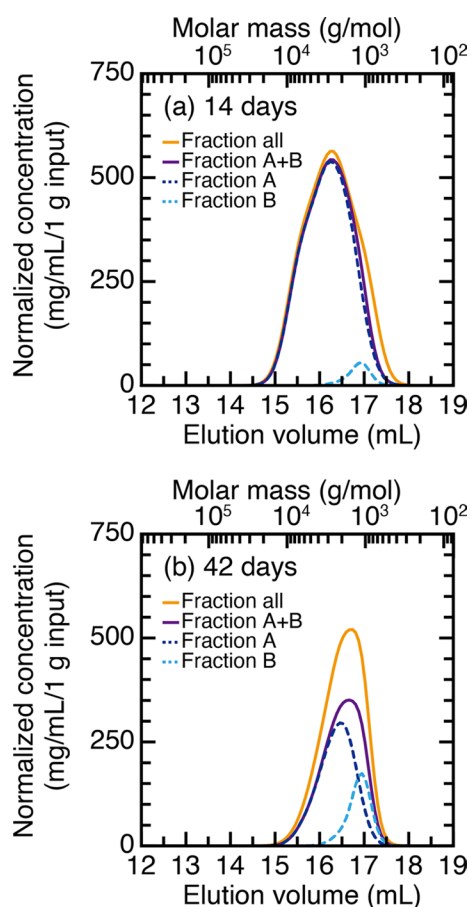


Fig. 4 SEC/MALLS elution patterns of “Fraction all”, “Fraction A+B”, “Fraction A”, and “Fraction B” at incubation periods of (a) 14 days and (b) 42 days. Normalized concentration (mg/mL/1 g input) was the concentration normalized by the yields as detailed in Supporting Information so as to visualize the transition of DPs and yields of each fraction. Molar mass at each elution volume is also shown on top of figures for clarity

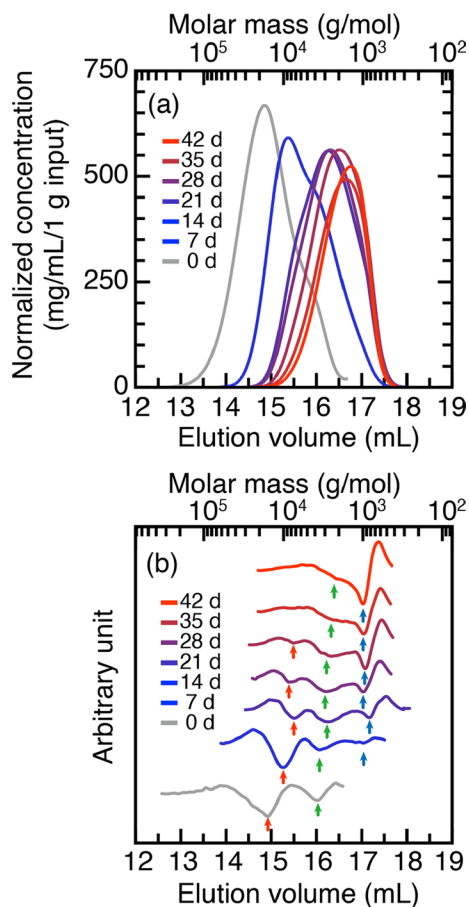


Fig. 5 a SEC/MALLS elution patterns of “Fraction all”. Incubation periods are shown in the figures. Normalized concentration (mg/mL/1 g input) was the concentration normalized by the yields as detailed in Supporting Information so as to visualize the transition of DPs and yields of each fraction. Molar mass at each elution volume is also shown on top of figures for clarity. **b** the second derivatives of Fig. 4a. Arrows correspond to the observed peaks that are denoted as Species 1 (red), 2 (green), and 3 (blue) in the ascending order of elution volume

3; corresponding DP: 6) gradually appeared. At 35 days of incubation, Species 1 disappeared or merged into Species 2 centered at 16.4 (corresponding DP: 14). The gradual shift of Species 1 and 2 toward lower molar mass supports not the hydrolysis at a specific length but the random hydrolysis. It should be noted that, as mentioned above, Species 3 was a simple byproduct given by the washing step, where the water-soluble cello-oligomers (DP less than 6) were eliminated.

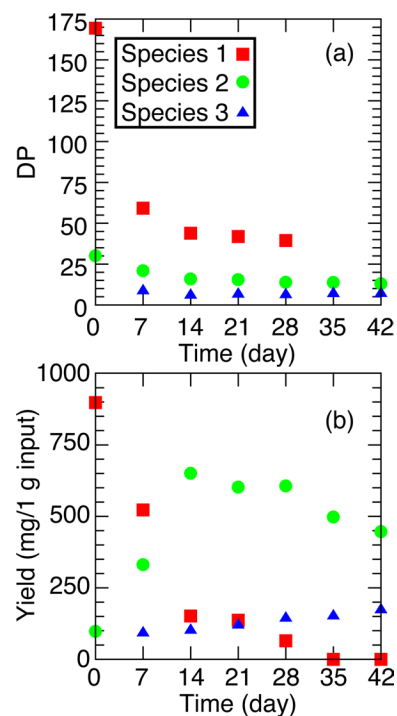


Fig. 6 Time course change of (a) DP and (b) yield of Species 1, 2, and 3 in the Fraction all. The detailed deconvolution process is given in Supporting Information

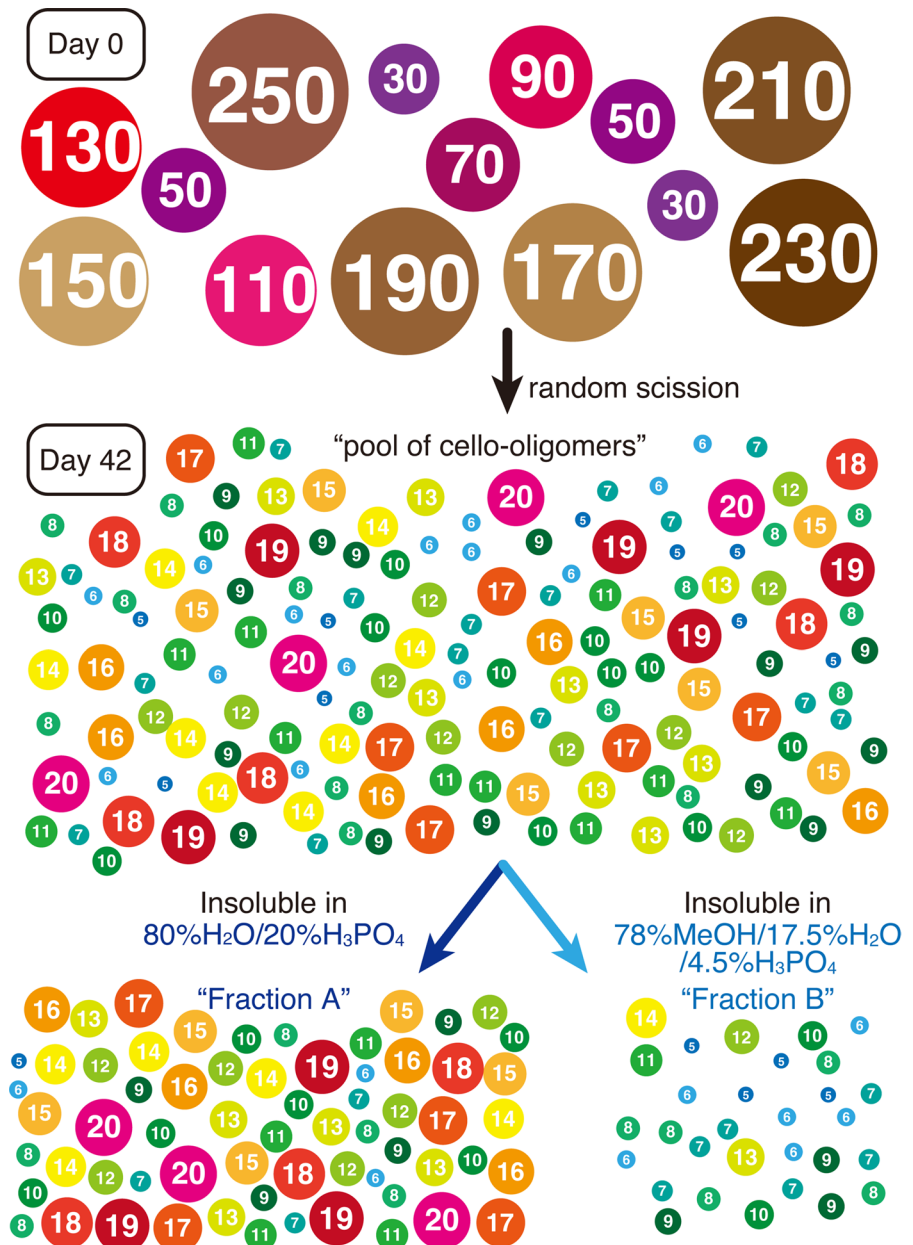
Speculation on the formation of mono-disperse cello-oligomers

Based on the number and position of downward concaves in the second derivatives, the deconvolution of SEC-MALLS patterns was conducted (for the detailed procedure and fitting results, see Supporting Information, Table S1, and Fig. S1). The DP of Species 1 and 2 decreased along the incubation time (Fig. 6a), while Species 3 had a constant DP of 7 from the first appearance (Table S1). The decrease in DP of Species 1 was slowed down from 14 days, where the DP reached around 40. Similarly, Species 2, DP lower than 30, showed a gradual decrease in DP from the beginning. This suggests that the rate of hydrolysis on the shorter chain was very slow. The reason behind this slow hydrolysis of short chain cellulose is unclear. The high rigidity of short chain cellulose is a possible explanation: the twist or kink, where the scission is likely, rarely appear on the elongated short-chain cellulose.

The yield of each species was obtained from the peak area (Fig. 6b). While Species 1 showed a monotonic decrease in yield, Species 2 initially showed an increase until 14 days of incubation and then gradually decreased in yield. Contrastingly, Species 3 showed gradual and linear increase from the first appearance. This temporal increase in the yield of Species 1 was due to the slower hydrolysis at short-chain cellulose.

From these findings, the speculated mechanism of mono-disperse cello-oligomers obtained from phosphoric acid hydrolysis is schematized in Fig. 7. The initial cellulose input contained two components with the DPw of 170 and 30. These components were subjected to the phosphoric acid hydrolysis, and the DP decreased through the random hydrolysis. However, the rate of hydrolysis became slower when the DP reached around 40, and the pool of cello-oligomers appeared. At 42 days, the DPs of most of pooled

Fig. 7 Schematic illustration of speculated mechanism of phosphoric acid hydrolysis. The numbers inside the circles correspond to the DPs, and the number of circles is based on each yield. Water-soluble cello-oligomers with the DP less than 4 are not included in this illustration



cello-oligomers became less than 20. By the solubility difference depending on the DP, the pool of cello-oligomers was fractionated into two: cello-oligomers with the DPw of 15 into water phase (80% H₂O / 20% H₃PO₄) and 8 into methanol phase (78% methanol/17.5% H₂O/4.5% H₃PO₄).

Conclusion

The formation of monodisperse cello-oligomers in the phosphoric acid was monitored quantitatively by SEC-MALLS. In the concentrated phosphoric acid solution, dissolved cellulose is gradually hydrolyzed and cello-oligomers with a DP 14–15 and 7–8 are selectively formed. Then, by adding water, DP 14–15 precipitates and DP less than 7–8 are soluble in the supernatant. By the subsequent addition of methanol into the supernatant, the fraction with DP less than 7–8 precipitates. By washing with water, cello-oligomers with DP less than 6 are washed away, and highly monodisperse cello-oligomer with DP 7–8 is recovered because of the insolubility in water. The selective formation of DP 14–15 can result from the slow rate of scission: the rate of hydrolysis becomes slower when the DP reached around 40, and there appears the pool of cell-oligomers, from which the DP 14–15 are fractionated by the use of solubility difference in aqueous 20 wt% H₃PO₄. The DP 7–8 originates from the water solubility of cello-oligomers with a DP less than 6 that are removed away during washing step. To address the mechanism behind the slow hydrolysis on the cello-oligomers, the hydrolysis at various conditions such as high or low temperature combined with *in-situ* observation such as small-angle X-ray or neutron scattering will be needed. In addition, to better understand the fractionation mechanism, the use of different precipitating agents such as salt solutions will be beneficial.

Author contributions NI conceived the concept of the study. NI, YO, YN, DR, and AI designed the experiments. NI and YO performed all experiments. All authors analyzed the data. NI wrote the first version of the manuscript, and all authors commented on previous versions of the manuscript. All authors read and approved the final manuscript.

Funding N.I. acknowledges support from the Grants-in-Aid for Scientific Research (KAKENHI Grant Nos. JP22H03786 and JP22K19885) from the Japan Society for the Promotion of Science (JSPS). This paper was partly based on the results

obtained from a project, JPNP18016 and PJ-ID 20001845, commissioned by the New Energy and Industrial Technology Development Organization (NEDO). This work received the financial support from the Institut Carnot PolyNat through the project RoCoCo. “Laboratoire Rhéologie et Procédés” (LRP) is a part of the LabEx Tec 21 (Investissements d’Avenir-grant agreement n° ANR-11-LABX-0030).

Declarations

Conflict of interest The authors declare no competing interests.

Ethical approval This article does not contain any studies with human participants or animals performed by any of the authors.

Open Access This article is licensed under a Creative Commons Attribution 4.0 International License, which permits use, sharing, adaptation, distribution and reproduction in any medium or format, as long as you give appropriate credit to the original author(s) and the source, provide a link to the Creative Commons licence, and indicate if changes were made. The images or other third party material in this article are included in the article’s Creative Commons licence, unless indicated otherwise in a credit line to the material. If material is not included in the article’s Creative Commons licence and your intended use is not permitted by statutory regulation or exceeds the permitted use, you will need to obtain permission directly from the copyright holder. To view a copy of this licence, visit <http://creativecommons.org/licenses/by/4.0/>.

References

- Buleon A, Chanzy H (1978) Single crystals of cellulose II. *J Polym Sci Polym Phys Ed* 16:833–839. <https://doi.org/10.1002/pol.1978.180160508>
- Cartier N, Domard A, Chanzy H (1990) Single crystals of chitosan. *Int J Biol Macromol* 12:289–294. [https://doi.org/10.1016/0141-8130\(90\)90015-3](https://doi.org/10.1016/0141-8130(90)90015-3)
- Cushen JD, Otsuka I, Bates CM et al (2012) Oligosaccharide/silicon-containing block copolymers with 5 nm features for lithographic applications. *ACS Nano* 6:3424–3433. <https://doi.org/10.1021/nn300459r>
- Fittolani G, Vargová D, Seeberger PH et al (2022) Bottom-Up approach to understand chirality transfer across scales in cellulose assemblies. *J Am Chem Soc* <https://doi.org/10.1021/jacs.2c04522>
- Hata Y, Sawada T, Sakai T, Serizawa T (2018) Enzyme-catalyzed Bottom-Up synthesis of mechanically and physicochemically stable cellulose hydrogels for spatial immobilization of functional Colloidal particles. *Biomacromolecules* 19:1269–1275. <https://doi.org/10.1021/acs.biomac.8b00092>
- Helbert W, Sugiyama J (1998) High-resolution electron microscopy on cellulose II and α -chitin single crystals.

- Cellulose 5:113–122. <https://doi.org/10.1023/A:1009272814665>
- Hiraishi M, Igarashi K, Kimura S et al (2009) Synthesis of highly ordered cellulose II in vitro using cellodextrin phosphorylase. *Carbohydr Res* 344:2468–2473. <https://doi.org/10.1016/j.carres.2009.10.002>
- Isogai A (1997) NMR analysis of cellulose dissolved in aqueous NaOH solutions. *Cellulose* 4:99–107
- Isogai A, Usuda M (1991) Preparation of low-molecular weight celluloses using phosphoric acid. *Mokuzai Gakkaishi* 37:339–344
- Jiang F, Zhang X, Hwang W et al (2021) Oligocellulose from acid hydrolysis: a revisit. *Appl Surf Sci* 537:1–6. <https://doi.org/10.1016/j.apsusc.2020.147783>
- Meiland M, Liebert T, Heinze T (2011) Tailoring the degree of polymerization of low molecular weight cellulose. *Macromol Mater Eng* 296:802–809. <https://doi.org/10.1002/mame.201000424>
- Muanprasat C, Chatsudthipong V (2017) Chitosan oligosaccharide: biological activities and potential therapeutic applications. *Pharmacol Ther* 170:80–97. <https://doi.org/10.1016/j.pharmthera.2016.10.013>
- Ono Y, Ishida T, Soeta H et al (2016) Reliable dn/dc values of cellulose, chitin, and cellulose triacetate dissolved in LiCl/N,N-Dimethylacetamide for molecular mass analysis. *Biomacromolecules* 17:192–199. <https://doi.org/10.1021/acs.biomac.5b01302>
- Oscarson S, Cheallaigh AN (2021) Strategies in oligosaccharide synthesis. *Compr Glycosci Second Ed* 52:1–48. <https://doi.org/10.1016/B978-0-12-819475-1.00075-4>
- Persson JE, Domard A, Chanzy H (1992) Single crystals of α -chitin. *Int J Biol Macromol* 14:221–224. [https://doi.org/10.1016/S0141-8130\(05\)80031-5](https://doi.org/10.1016/S0141-8130(05)80031-5)
- Perugino G, Trincone A, Rossi M, Moracci M (2004) Oligosaccharide synthesis by glycosynthases. *Trends Biotechnol* 22:31–37. <https://doi.org/10.1016/j.tibtech.2003.10.008>
- Seeberger PH (2008) Automated oligosaccharide synthesis. *Chem Soc Rev* 37:19–28. <https://doi.org/10.1039/b511197h>
- Serizawa T, Fukaya Y, Sawada T (2017) Self-Assembly of cellulose oligomers into nanoribbon network structures based on kinetic control of enzymatic oligomerization. *Langmuir* 33:13415–13422. <https://doi.org/10.1021/acs.langmuir.7b03653>
- Talsky G, Mayring L, Kreuzer H (1978) High-Resolution, higher-order UV/VIS derivative spectrophotometry. *Angew Chemie Int Ed English* 17:785–799. <https://doi.org/10.1002/anie.197807853>
- Taylor JB (1957) The water solubilities and heats of solution of short chain cellulosic oligosaccharides. *Trans Faraday Soc* 53:1198. <https://doi.org/10.1039/tf9575301198>
- Yataka Y, Sawada T, Serizawa T (2015) Enzymatic synthesis and post-functionalization of two-dimensional crystalline cellulose oligomers with surface-reactive groups. *Chem Commun* 51:12525–12528. <https://doi.org/10.1039/c5cc04378f>
- Zhang X, Jiang F, Torres-Luna C et al (2021) Solvent-assisted fractionation of oligomeric cellulose and reversible transformation of cellulose II and IV. *ACS Biomater Sci Eng* <https://doi.org/10.1021/acsbiomaterials.1c00885>

Publisher's Note Springer Nature remains neutral with regard to jurisdictional claims in published maps and institutional affiliations.